Ain Shams Engineering Journal 14 (2023) 101992

Contents lists available at ScienceDirect

Ain Shams Engineering Journal

journal homepage: www.sciencedirect.com

Thinned-out controlled IC MPPT algorithm for class E resonant inverter with PV system

Akif Karafil

Department of Electrical and Electronics Engineering, Engineering Faculty, Yalova University, Yalova, Turkey

ARTICLE INFO

Article history:
Received 2 September 2021
Revised 15 May 2022
Accepted 12 September 2022
Available online 30 September 2022

Keywords:
Thinned-out control
IC MPPT
Class E resonant inverter
Zero voltage switching

ABSTRACT

In this study, maximum power extracted from photovoltaic (PV) panels was transferred to the load using the proposed thinned-out controlled class E resonant inverter. For the system, PV panels were used as a power source. A PV powered system was designed using single switch inverter. Maximum power point tracker (MPPT) controlled resonant inverter was conducted under varying solar irradiation conditions. The output power of the voltage-fed class E resonant inverter circuit was controlled in a wide range by using the thinned-out control method in a fixed switching frequency of 63 kHz. In the proposed method, power control was provided gradually without increasing switching losses significantly by achieving zero voltage switching (ZVS) condition. ZVS conditions were met in most periods when the solar irradiation was at high level and the number of the skipped pulses was low. As a result, soft switching was provided and the single switch inverter could operate with higher efficiency. Incremental conductance (IC) algorithm was used to track maximum power in PV panels and the tracking efficiency was obtained as above 99 % by the proposed novel thinned-out controlled IC MPPT algorithm. The proposed method shows that since electromagnetic interference and switching losses are reduced, the size of the circuit components is also reduced, and therefore there is a significant reduction in the circuit volume and the costs.

1. Introduction

Due to the gradual increase in the production in the mechanized industry, the demand for electrical energy has also increased day by day. Although most of the electrical energy is still generated by fossil-based sources such as oil and coal, there has been considerable interest in alternative energy sources recently since the gases produced from burning of fossil-based resources pollute the environment and these resources will run out in the near future. Today, renewable energy sources such as solar, wind, geothermal, biomass are frequently used as alternative energy sources [1,2]. In order to compete with fossil-based sources, solar energy, which is one of the major renewable energy sources, has become more prominent with recent researches, projects and investments [3].

The most important advantages of photovoltaic (PV) systems, in which electrical energy is generated by utilizing solar energy, are that they are simple to install, do not need much maintenance and can provide power up to megawatts. Additionally, the widespread use of PV pumping systems, solar home systems, and off-grid buildings increases the demand for PV energy. However, the low efficiency of the PV panel, the change in atmospheric conditions during the day and the constant change in the power values obtained from the PV panels are the main drawbacks of PV energy systems [4]. Therefore, maximum power point tracker (MPPT) converters are utilized to get the maximum solar energy from PV panels. Rather than being a mechanical tracking system that provides the tracking of solar by moving PV panels physically, MPPT is an electronic system that provides extracting maximum possible power from PV panels. When the literature is examined, it is seen that there are many MPPT algorithms used in determining maximum power point (MPP). Perturb & Observe (P&O) and Incremental Conductance (IC) algorithms, which have high MPP tracking efficiency, are the two important algorithms. Especially IC MPPT

Peer review under responsibility of Ain Shams University.
E-mail address: akif.karafil@yalova.edu.tr

Production and hosting by Elsevier

https://doi.org/10.1016/j.asej.2022.101992
2090-4479/

algorithm is frequently used due to its high tracking efficiency, less oscillation around the MPP and being robust in harsh atmospheric conditions [5]. MPPT based PV systems are commonly used in various fields such as storage systems [6], grid connected applications [7] and induction heating systems [8].

Today, power converters are used in many applications such as uninterruptible power supplies, electronic ballasts, wireless power transfer, induction heating. The development of semiconductor elements used in power converters has enabled the converters to operate at higher frequencies. Efficiency is increased by reducing the size of electronic circuits by operating at high frequencies. In order to operate at high frequency, the switching losses must be low. Reduction of switching losses by preventing electromagnetic interference is provided by resonant power converters. Resonant power converter is obtained by adding inductance (L) and capacitor (C) elements to the switch element. In resonant power converter circuits, switching is carried out at zero or near zero crossing of the current passing through the switch or the voltage at the ends of the switch. In this way, switching losses are reduced and the circuit is operated at high frequencies [9,10].

In DC/AC power converters, full and half bridge inverters are used, as well as single-switch inverter types. Since two or four switches are used in bridge type inverter circuits, the circuit structure becomes more complex and the costs increase. In such circuits, the efficiency is higher and high output power and power control in desired ranges can be achieved. By using soft switching techniques, switching losses can be reduced using single switch resonant inverters. Class E inverters in the group of single-switch power converters can increase the efficiency of the circuit by reducing the switching losses when soft switching conditions are met. In addition, since the number of elements used in the circuit decreases, the structure of such circuits is simple, the cost is lowered, and the volume is reduced. The main drawback of class E inverters is that the switch voltage and current are higher than the source voltage and current. Therefore, it is required to use a power switch with a higher value [11–13].

Various control techniques such as phase shift [14], frequency modulation [15], pulse width modulation (PWM) [16] and duty cycle control [17] are used in class E inverters to control the power transferred to the load. Besides these control techniques, thinned-out control method also provides power control. In the thinned-out control method, power control is provided by skipping some of the pulses at a fixed operating frequency without any change in the transmission time of the switch. The power decreases as the transmission pulses are skipped [18–20]. Thinned-out control method are used in applications such as induction cooking applications [21], corona discharge process [22], medical devices [23], wireless power transfer systems [24], PV systems [25] and dimming electronic ballasts [26].

In the literature, Sensui and Koizumi [27] analyzed the load independent zero voltage switching (ZVS) parallel resonant inverter circuit. Kaczmarczyk and Jurczak [28] improved the efficiency of a push–pull circuit by reducing the switching losses by achieving the ZVS condition. Zhang and Ngo [29] analyzed the constant current ZVS class E inverter topology by keeping the duty cycle and switching frequency constant under load changes. Roslaniec et al. [30] examined class E inverter structure in which wide range variable load resistance ZVS condition was provided. Issi and Kaplan [31] performed the wireless energy transfer using the class E inverter by meeting the ZVS condition. Shigeno and Koizumi [32] applied the thinned-out control method to the half-wave class DE rectifier circuit. Koizumi et al. [33] used the thinned-out control method in the resonant DC/DC converter circuit.

When the literature is examined, it is seen that ZVS conditions have been achieved and thinned-out control method has been applied for different applications. However, thinned-out controlled IC MPPT algorithm has not been utilized for PV powered class E resonant inverter. In this study, the simulation of a MPPT system with class E resonant inverter that transfers the electrical power extracted from PV panels to the load appropriate for the system was carried out by using the proposed thinned-out control method. Thinned-out controlled MPPT was used to control the single switch inverter that can operate at 63 kHz switching frequency under varying solar irradiation conditions for PV panels. In the proposed thinned-out controlled MPPT, the number of the skipped pulses were increased and decreased to control the power. By providing ZVS conditions in many periods, it was ensured that the system could operate at high frequency. The total power of the PV panels was 360 W. In the study, IC algorithm was preferred as the MPPT method in order to keep the output power obtained from PV panels continuously at maximum level because of its high efficiency.

2. The analysis of thinned-out controlled class E resonant inverter

2.1. Voltage-fed class E resonant inverter

Conventional class E resonant inverter requires DC source. When class E resonant inverter is fed by a PV source, PV energy can be transferred to the load without being converted to DC. In Fig. 1, voltage-fed class E resonant inverter circuit is shown. The circuit consists of a switch element (S), resonant inductance (L_r), resonant capacitor (C_r) and a series resistance (R). Since the number of elements in the circuit is decreased, the circuit has a simple structure, smaller size, and it is low cost. In this circuit, the switch can be turned on and off with zero voltage.

As long as the S switch is on in the circuit, the inductance current increases and energy is stored. Capacitor voltage is zero as long as the switch is on. A series RLC circuit is formed when the switch is off. In this case, the inductance current and capacitor voltage are in the form of damped oscillations. As long as the switch is off, the capacitor voltage reaches its peak value and drops back to zero. When the capacitor voltage takes a negative value, the energy stored in the inductance is transferred to the source via the diode connected in reverse parallel to the switch element, ensuring that the capacitor voltage remains at its zero value. In this way, it is ensured that the switch is on due to zero voltage. Fig. 2 presents waveforms of control signal (S), inductance current (i_L) and capacitor voltage (V_C) in the ZVS condition.

Voltage-fed Class E resonant inverter circuit can be examined in four states according to the on and off position of the switch.

2.1.1. State I ($t_0 < t < t_1$)

As can be seen in Fig. 2, State I is between the range of $t_0 < t < t_1$ and the switch is on. Since the switch is on, the resistance and

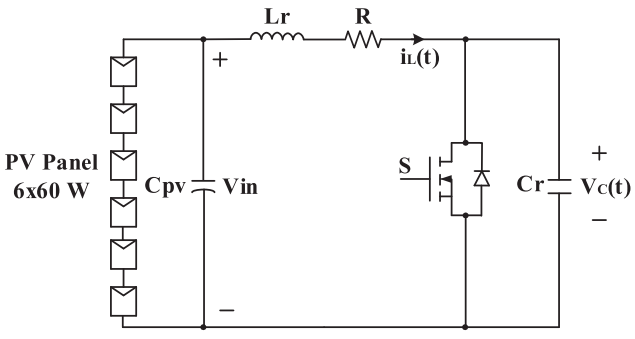

Fig. 1. Class E resonant inverter circuit.

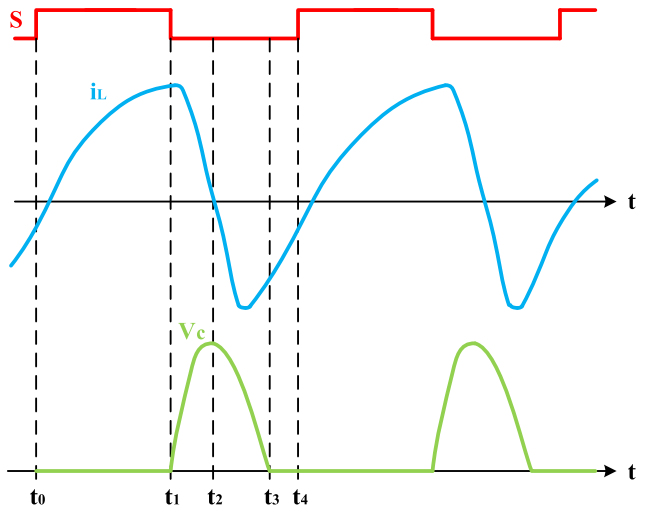

Fig. 2. The control signal (S), inductance current (i_L) and capacitor voltage (V_C) in the ZVS condition.

inductance are connected in series and the voltage of the capacitor is zero. The equivalent circuit of State I is presented in Fig. 3.

Depending on the initial current, the value of the inductance current changes depending on the time constant (τ) when the switch is on. The time constant and current equations can be calculated using the following equations.

$$\tau = \frac{L_r}{R} \tag{1}$$

$$i_L(t) = \frac{V_{in}}{R} + \left(i(t_0) - \frac{V_{in}}{R}\right)e^{-\frac{t}{\tau}} \tag{2}$$

2.1.2. State II ($t_1 < t < t_2$)

As can be seen in Fig. 2, State II is in the range of $t_1 < t < t_2$ and the switch is off. In this situation, resistance, inductance and capacitor are connected in series. The equivalent circuit of State II is presented in Fig. 4.

Capacitor voltage is at its maximum value at t_2. At this moment, the inductance current is zero. Capacitor voltage and inductance current equations are obtained by the following equations.

$$V_c(t) = V_{in} - Ri_L(t) - L\frac{di_L(t)}{dt} \tag{3}$$

$$i_L(t) = C_r\frac{dV_c(t)}{dt} \tag{4}$$

2.1.3. State III ($t_2 < t < t_3$)

In State III, the switch is off and the capacitor's energy is transferred to the source. The equivalent circuit of State III is shown in Fig. 5.

The characteristic roots of the circuit depend on the resonant angular frequency (ω_o) and damping factor (ξ).

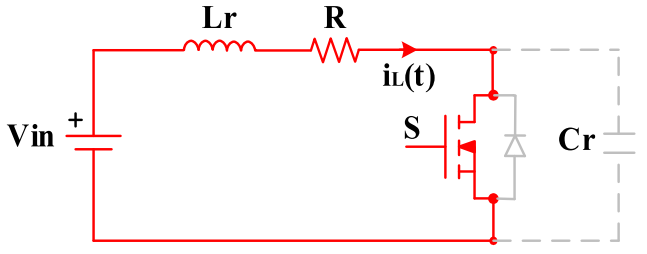

Fig. 3. The equivalent circuit of State I.

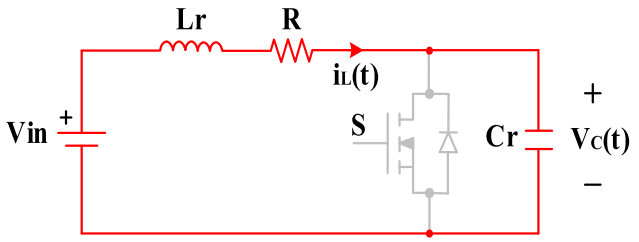

Fig. 4. The equivalent circuit of State II.

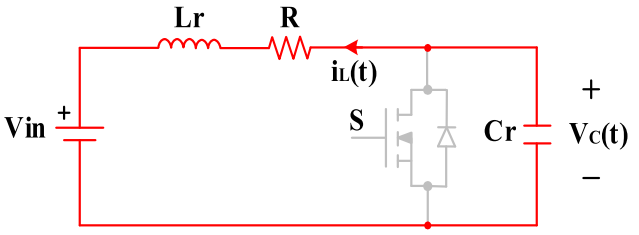

Fig. 5. The equivalent circuit of State III.

$$\omega_o = \frac{1}{\sqrt{L_rC_r}} \tag{5}$$

$$\xi = \frac{R}{2L_r} \tag{6}$$

When $\xi < \omega_o$ in the circuit, the roots are in complex conjugate and damped oscillation occurs. Since the energy in the circuit is consumed through the resistance, the inductance current and capacitor voltage are in the form of damped oscillations. The damped oscillation value of the inductance current is calculated by the following equation.

$$i_L(t) = e^{-\xi t}(A_1 \sin\omega_n t + A_2 \cos\omega_n t) + B \tag{7}$$

The coefficients A_1 and A_2 represent the initial conditions, while the B value is the steady-state solution of the inductance current. The ω_n in the equation is the natural angular frequency.

$$A_1 = \frac{V_{in} - RI_0}{L_r\omega_n} + \frac{\xi I_0}{\omega_n} \tag{8}$$

$$A_2 = I_0 \tag{9}$$

$$\omega_n = \sqrt{\omega_o^2 - \xi^2} \tag{10}$$

Another important parameter is the load quality factor (Q). If the load quality factor is not high enough, the inductance current and capacitor voltage values are damped and the current value drops to zero. The load quality factor is calculated by the following equation.

$$Q = \frac{\omega_o L_r}{R} \tag{11}$$

2.1.4. State IV ($t_3 < t < t_4$)

The capacitor voltage is zero at t_3. The energy in the inductance is transferred to the source via the diode connected in reverse parallel to the switch element. The equivalent circuit of State IV is given in Fig. 6.

The value of the inductance current is calculated by the following equation.

$$i_L(t) = \frac{V_{in}}{R} + \left(i(t_3) - \frac{V_{in}}{R}\right)e^{-\frac{t}{\tau}} \tag{12}$$

When the time intervals of State I, II, III and IV are considered, the rms value of the inductance current and the power that will be consumed by the resistance can be calculated [21,34,35].

$$I_{L(rms)} = \sqrt{\frac{1}{T_{sw}}\left[\int_0^{T_{sw}} (i_L(t))^2 dt\right]} \quad (13)$$

$$P = \left(I_{L(rms)}\right)^2 R \quad (14)$$

2.2. Proposed thinned-out control method

Various control methods such as PWM, frequency, phase shift, etc. are widely used to control the inverters. However, these control methods have some drawbacks such as switching loss, failure to perform a wide range of power control and failure to operate at a fixed frequency. On the other hand, PV panels cannot produce the same power all the time. Therefore, class E resonant inverter cannot operate at a fixed operation frequency with these control methods. On the contrary, the thinned-out control method can ensure that the power can be controlled with fixed operating frequency using a class E resonant inverter by providing ZVS conditions.

The thinned-out control method consists of a set of commands, which provides power control when some of the control pulses are skipped based on the command sequences with no change in switching frequency and turn on duration of the switch [20,36]. Fig. 7 presents the proposed thinned-out switching patterns.

When the maximum switching pattern length 8 is chosen, thinned-out ratio will vary from 1/8 to 8/8. When the thinned-out ratio is 1/8, the power is at the lowest level and the power is at maximum level in 8/8. In other words, as the pulse numbers are skipped, the power ratio decreases. The thinned-out ratio (T_{or}) is defined as;

$$T_{or} = \frac{M - X}{M} \quad (15)$$

where M is the total number of pulses and X is the number of thinned-out pulses.

Although operating frequency and input voltage of thinned-out controlled inverters are fixed, the inverter is operated in four different switching stages to adjust the output power. The control scheme of the proposed thinned-out control method is presented in Fig. 8. As seen in the Figure, the thinned-out ratio is 6/8 (11101110) and 2 pulses are skipped while 6 pulses are not skipped. Since the switch element and the capacitor are connected in parallel in this circuit, the capacitor voltage is also the voltage at the switch ends. Although the ZVS conditions cannot be achieved after the thinned-out pulse part, the efficiency of the inverter is high as the ZVS conditions are provided in many switching periods.

Inductance current and capacitor voltage continue to oscillate in thinned-out pulse intervals. The rms value of the damped oscillation current decreases depending on the increase in the number of thinned-out pulses. If the number of thinned-out pulses increases and the duration is long, the inductance current drops to zero while the capacitor voltage drops to the input voltage value [18–21].

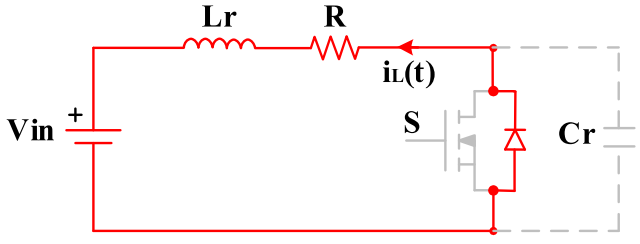

Fig. 6. The equivalent circuit of State IV.

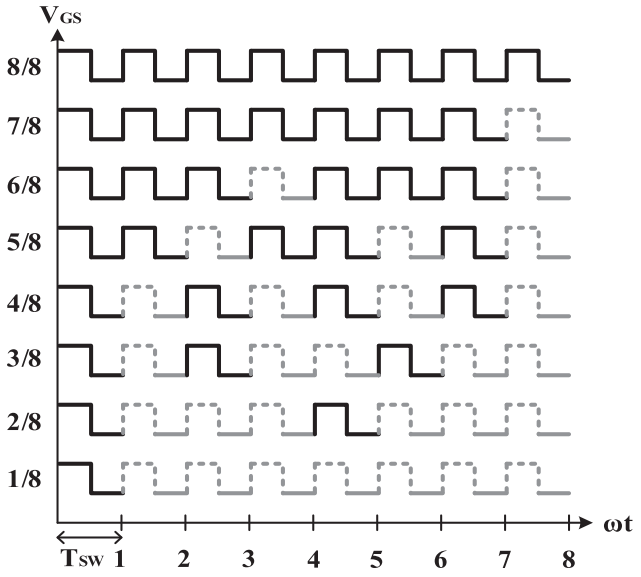

Fig. 7. The proposed thinned-out switching patterns.

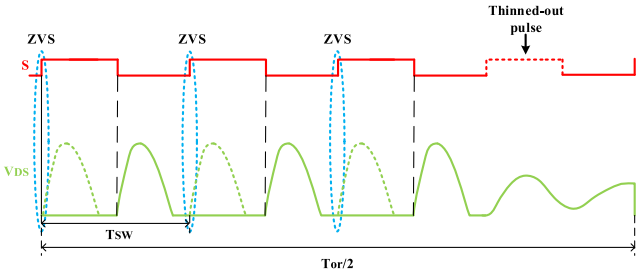

Fig. 8. The basic structure of the proposed thinned-out control method.

3. Thinned-out controlled IC MPPT algorithm

Block scheme of the thinned-out controlled IC MPPT system is shown in Fig. 9.

The catalog values of a polycrystalline PV panel used in the system are given in Table 1.

A total of 360 W power was obtained by connecting six panels with same properties in series. I-V and P-V characteristics of PV panels were investigated at 25 °C and 250–500–750 and 1000 W/m^2 solar irradiation (see Fig. 10).

Some disturbance may occur in the voltage and current values measured from the PV panels. In the system, low pass filter (LPF) was preferred to ensure that maximum power point could be tracked accurately by removing these disturbances. Thinned-out controlled IC MPPT algorithm flowchart is presented in Fig. 11.

IC MPPT method is based on the principles that PV panel P-V characteristic curve slope is zero at MPP (dP/dV = 0), positive on the left of MPP (dP/dV > 0) and negative on the right of MPP (dP/dV < 0). In the first step, current and voltage of the PV panel are measured and the obtained values are compared with the previous ones. Next, instantaneous rate of current (In) and voltage (Vn) are obtained and it is checked whether voltage change (dV) is zero or not. If dV is equal to zero and the current change (dI) is positive (dI > 0), pulses are not skipped. If dV is equal to zero but dI is neg-

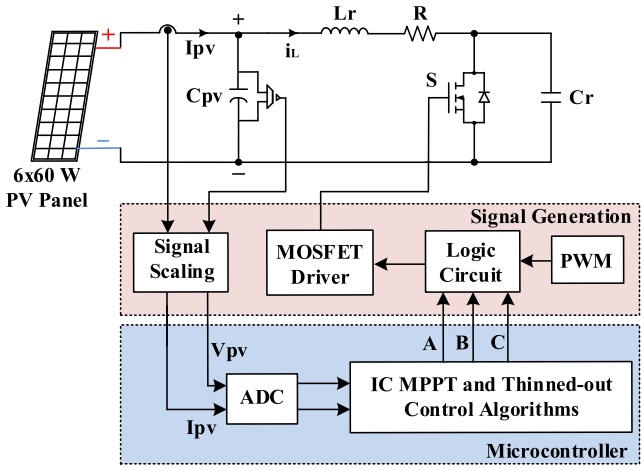

Fig. 9. Block scheme of the thinned-out controlled IC MPPT system.

Table 1
Catalog values of PV panel.

Electrical properties of PV panel	Values
Maximum power (P_{max})	60 W
Maximum power voltage (V_{mpp})	17.1 V
Maximum power current (I_{mpp})	3.5 A
Open circuit voltage (V_{oc})	21.1 V
Short circuit current (I_{sc})	3.8 A
Temperature coefficient of open circuit voltage	−(80 ± 10) mV/°C
Temperature coefficient of short circuit current	(0.065 ± 0.015) %/°C

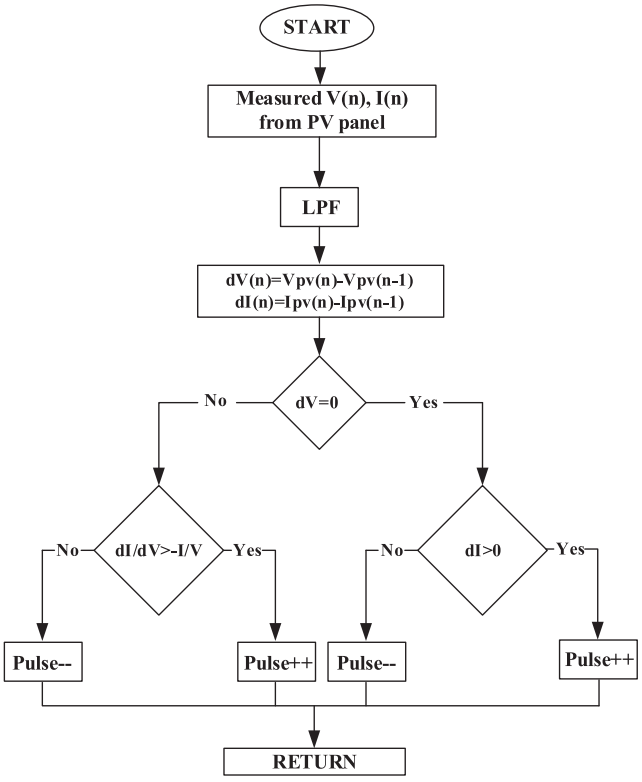

Fig. 11. Flowchart of the thinned-out controlled IC MPPT algorithm.

ative (dI < 0), pulses are skipped. If dV is not equal to zero and dI/dV is bigger than -I/V (dI/dV > -I/V), pulses are not skipped. If dI/dV is smaller than -I/V (dI/dV < -I/V), pulses are skipped. As a result, thinned-out control method makes it possible to obtain maximum power from the PV panel and to transfer maximum power to the load.

4. Simulation results

In this study, the simulation study was conducted using PSIM program for thinned-out controlled MPPT system in terms of MPPT efficiency and ZVS conditions. Solar irradiation level was rapidly changed step by step as 250–500–750 and 1000 W/m^2. In this way, thinned-out controlled IC MPPT algorithm was tested. The total power of the system was 360 W and six PV panels of 60 W were connected in series. Resonant frequency of the circuit was 108 kHz. In order for the inverter circuit to operate normally, there is a lower limit value for the on time of the switch. Since the capacitor voltage cannot reach zero value when a value lower than the limit value is obtained, the ZVS condition cannot be provided. When the off time of the switch is long, the end value of the inductance current becomes zero and the rms value decreases. Considering all these situations, the switching frequency of the circuit was

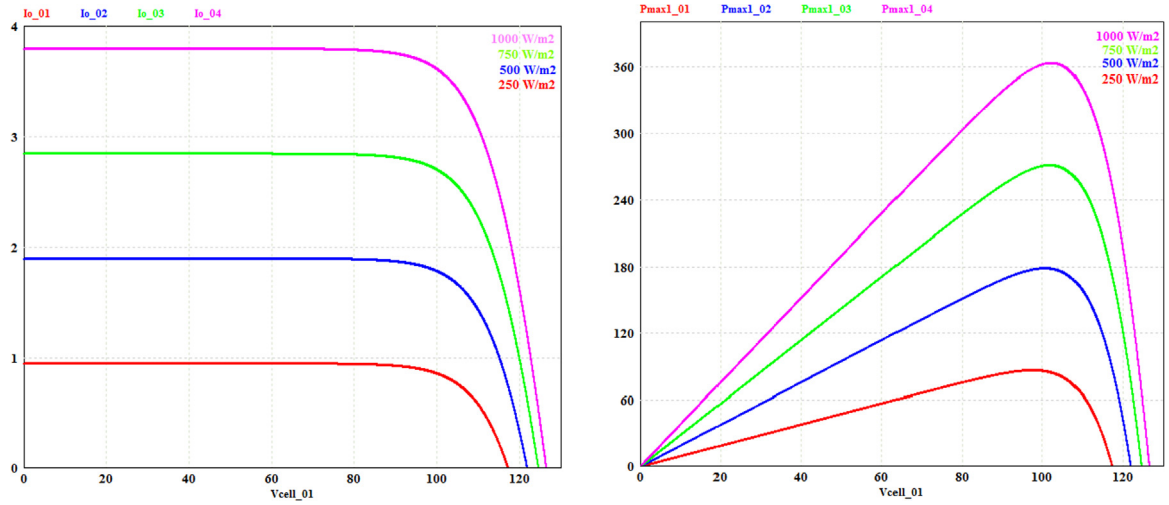

Fig. 10. I-V and P-V characteristics under varying solar irradiation.

determined as 63 kHz. The circuit parameters were selected as 30 μH resonant inductor, 72 nF resonant capacitor, 3.2 Ω load resistance. The simulation image of the thinned-out controlled IC MPPT system is given in Fig. 12.

The theoretical PV power (P_{ref}) and the output power of PV panel obtained according to MPPT algorithm (P_{mppt}) from the proposed system is shown in Fig. 13.

As can be seen in Fig. 13, the desired P_{mppt} power settling time is fast and the oscillation around the MPP is less. Additionally, the MPPT efficiency is over 99 %. The change of thinned-out pulses depending on the variation of solar irradiation is given in Fig. 14.

The simulation images of the control signal of switch, inductance current and capacitor voltage for 500 W/m^2 solar irradiation are presented in Fig. 15.

Maximum power was obtained from PV panels at 500 W/m^2 solar irradiation when the thinned-out ratio was 4/8. As can be seen in Fig. 15, 4 control pulses were skipped depending on the power value that PV panel required, and panels were operated at MPP.

The simulation images of the control signal of switch, inductance current and capacitor voltage for 750 W/m^2 solar irradiation are presented in Fig. 16.

Maximum power was obtained from PV panels at 750 W/m^2 solar irradiation when the thinned-out ratio was 6/8. As can be seen in Fig. 16, 2 control pulses were skipped depending on the power value that PV panel required, and panels were operated at MPP. In addition, it is seen that the ZVS conditions were provided in many periods.

The simulation images of the control signal of switch, inductance current and capacitor voltage for 1000 W/m^2 solar irradiation are presented in Fig. 17.

Maximum power was obtained from PV panels at 1000 W/m^2 solar irradiation when the thinned-out ratio was 8/8. As can be seen in Fig. 17, no control pulses were skipped depending on the

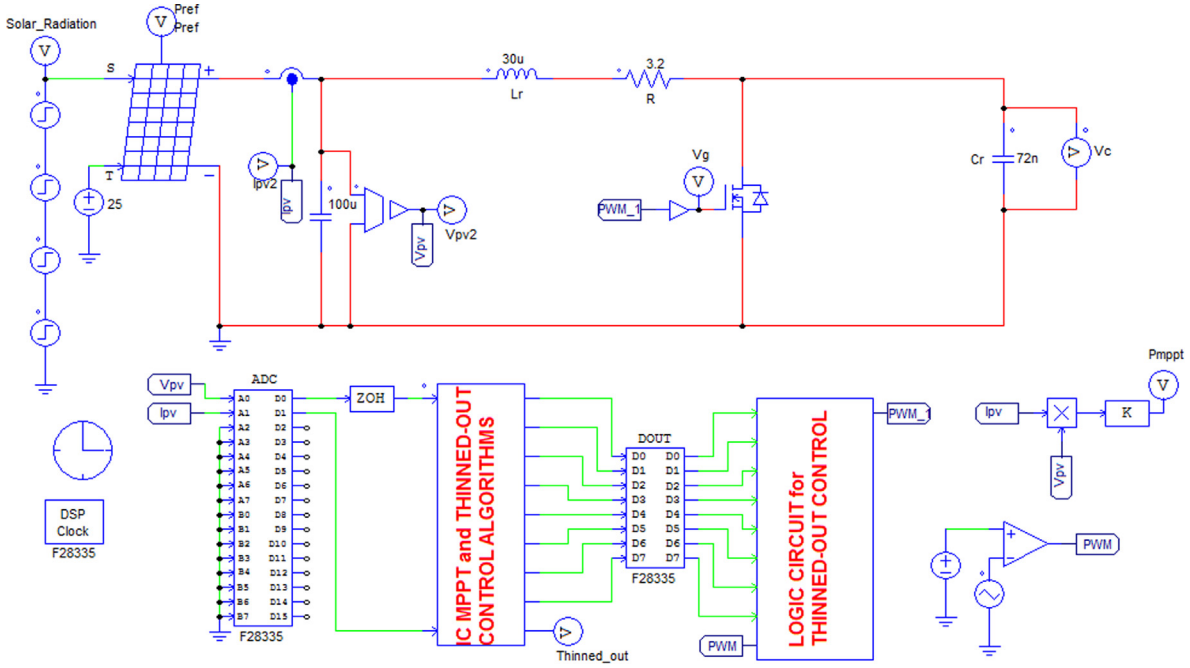

Fig. 12. Simulation image of the thinned-out controlled IC MPPT system.

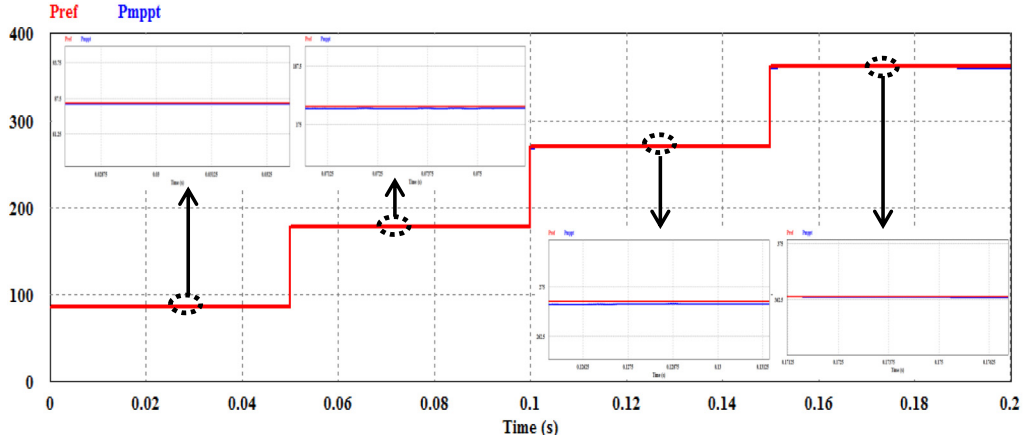

Fig. 13. The power tracking of thinned-out controlled IC MPPT algorithm.

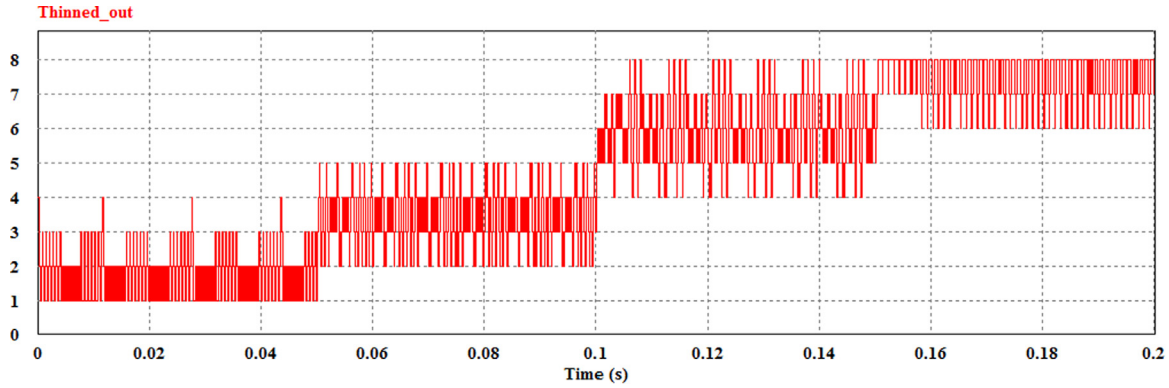

Fig. 14. The change of thinned-out pulses depending on the variation of solar irradiation.

power value that the PV panel required, and panels were operated at MPP. In addition, the ZVS conditions were provided in many periods.

The simulation results showed that in the test study of a PV powered single switch inverter conducted at different level of solar irradiation values, the tracking efficiency of the thinned-out controlled IC MPPT algorithm was found to be over 99 %. The switching frequency was as 63 kHz and constant in all results. The maximum power generated by PV panels was sent to the load. Especially in high solar irradiation levels, the ZVS condition was provided in many periods, which has reduced the losses and increased the efficiency.

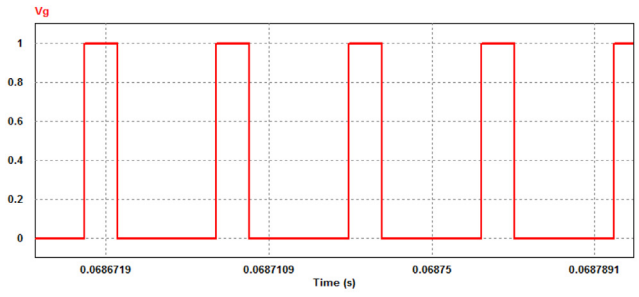

(a) Control signal of switch

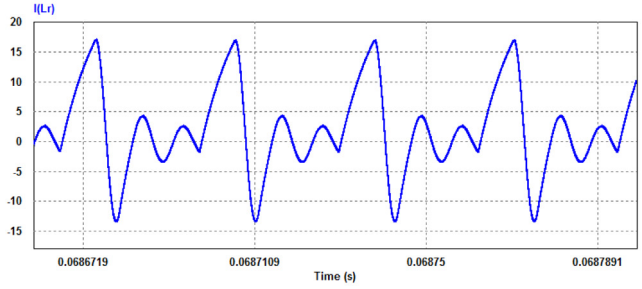

(b) Inductance current

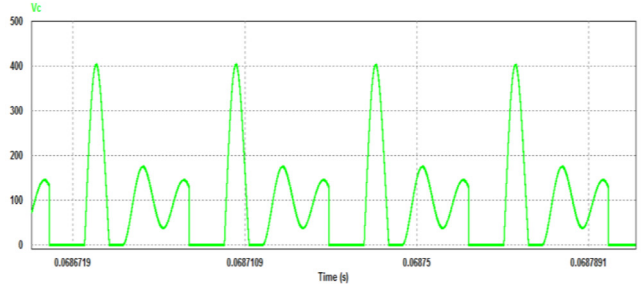

(c) Capacitor voltage

Fig. 15. Values obtained at 500 W/m^2 solar irradiation.

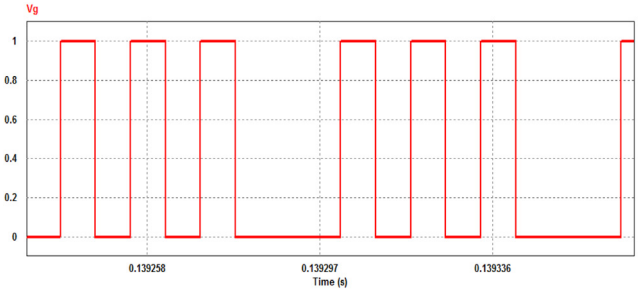

(a) Control signal of switch

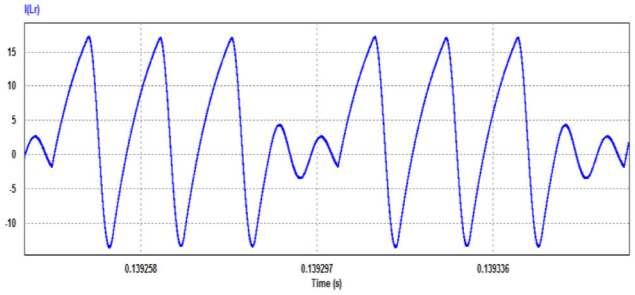

(b) Inductance current

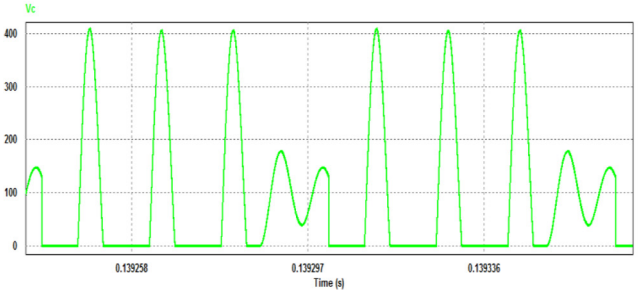

(c) Capacitor voltage

Fig. 16. Values obtained at 750 W/m^2 solar irradiation.

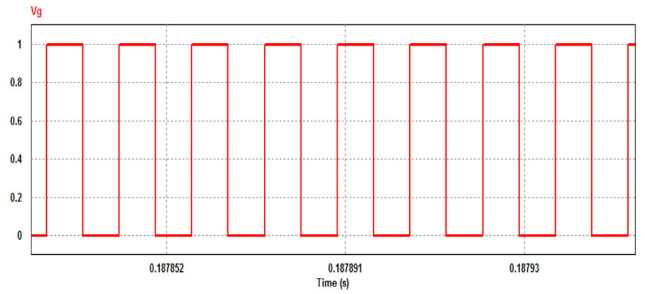

(a) Control signal of switch

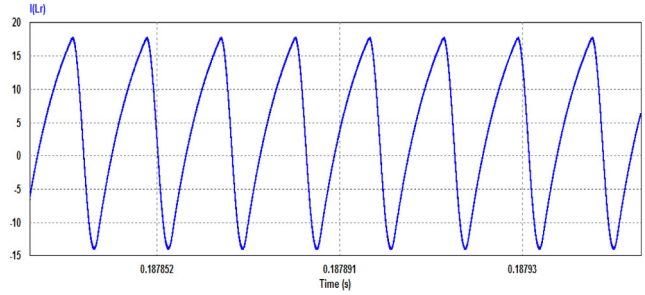

(b) Inductance current

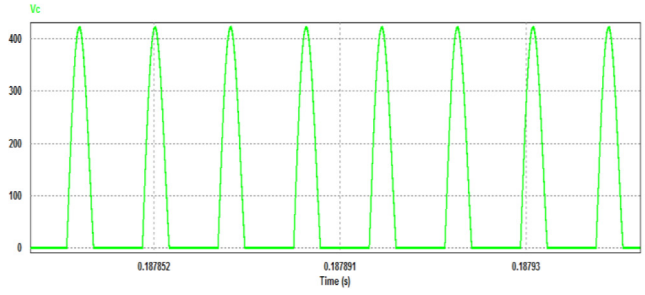

(c) Capacitor voltage

Fig. 17. Values obtained at 1000 W/m^2 solar irradiation.

5. Conclusion

In this study, thinned-out controlled IC MPPT algorithm, which is a new control method based on adjusting the varying solar irradiation values, was tested and tracking efficiency was found as over 99 %. It was seen that the settling time of the desired power value was both fast and there was no excessive oscillation around the MPP. Then the energy generated through PV panels was sent to the load. The proposed thinned-out controlled PV powered class E resonant inverter was realized at 63 kHz fixed switching frequency. Especially in high solar irradiation values, ZVS conditions were provided in many periods. As a result, higher operating frequency was provided and hard switching conditions, which are the main drawbacks of the conventional PWM switched MPPTs, were overcome. With the proposed thinned-out controlled MPPT algorithm, the power control was provided by adjusting the pulse skip. This study has a total power of 360 W, and it can be used in many applications such as induction heating, electronic ballast, etc. In the following studies, different MPPT algorithms (P&O, fuzzy logic etc.) can be tested and compared with each other by using the thinned-out control method on the same circuit topology. In addition, the proposed method can be applied to different renewable energy systems such as wind and hybrid PV/wind, which require low power. A class E zero current switching inverter circuit topology can be analyzed, similar circuit topologies can be examined, and more comprehensive studies can be conducted by using the different thinned-out pattern structure.

Declaration of Competing Interest

The authors declare that they have no known competing financial interests or personal relationships that could have appeared to influence the work reported in this paper.

References

[1] Hemeida AM, El-Ahmar MH, El-Sayed AM, Hasanien HM, Alkhalaf S, Esmail MFC, et al. Optimum design of hybrid wind/PV energy system for remote area. Ain Shams Eng J 2020;11(1):11–23.
[2] Bayindir R, Yesilbudak M, Colak M, Genc N. A novel application of naive bayes classifier in photovoltaic energy prediction. In: 2017 16th IEEE international conference on machine learning and applications (ICMLA), Cancun, Mexico, 18-21 Dec. 2017. p. 523-7.
[3] Loukil K, Abbes H, Abid H, Abid M, Toumi A. Design and implementation of reconfigurable MPPT fuzzy controller for photovoltaic systems. Ain Shams Eng J 2020;11(2):319–28.
[4] Mirza AF, Ling Q, Javed MY, Mansoor M. Novel MPPT techniques for photovoltaic systems under uniform irradiance and Partial shading. Sol Energy 2019;184:628–48.
[5] Mao M, Cui L, Zhang Q, Guo K, Zhou L, Huang H. Classification and summarization of solar photovoltaic MPPT techniques: A review based on traditional and intelligent control strategies. Energy Rep 2020;6:1312–27.
[6] Akeyo OM, Rallabandi V, Jewell N, Ionel DM. The design and analysis of large solar PV farm configurations with DC-Connected battery systems. IEEE Trans Ind Appl 2020;56(3):2903–12.
[7] Karafil A, Ozbay H, Oncu S. Design and analysis of single-phase grid-tied inverter with PDM MPPT-controlled converter. IEEE Trans Power Electron 2020;35(5):4756–66.
[8] Özbay H, Karafil A, Öncü S. Sliding mode PLL-PDM controller for induction heating system. Turk J Elec Eng Comp Sci 2021;29(2):1241–58.
[9] Reatti A, Corti F, Pugi L, Kazimierczuk MK, Migliazza G, Lorenzani E. Control strategies for Class-E resonant inverter with wide load variation. In: 2018 IEEE International Conference on Environment and Electrical Engineering and 2018 IEEE Industrial and Commercial Power Systems Europe (EEEIC/I&CPS Europe), Palermo, Italy, 12-15 June 2018. p. 1-6.
[10] Neogi K, Sadhu M, Das N, Sadhu PK, Chakraborty A, Ganguly A, et al. A new approach for the stability analysis of high-frequency series resonant inverter-fitted induction heater. Ain Shams Eng J 2019;10(1):185–94.
[11] Sarnago H, Lucia O, Mediano A, Burdio JM. A class-E direct ac–ac converter with multicycle modulation for induction heating systems. IEEE Trans Ind Electron 2014;61(5):2521–30.
[12] Ekbote A, Zinger DS. Comparison of class E and half bridge inverters for use in electronic ballasts. In: Conference Record of the 2006 IEEE Industry Applications Conference Forty-First IAS Annual Meeting, Tampa, Florida, USA, 8-12 Oct. 2016. p. 2198-201.
[13] Saito S, Mita S, Zhu W, Onishi H, Nagaoka S, Uematsu T, et al. Novel design approach of soft-switching resonant converter with performance visualization algorithm. IEEE Access 2020;8:59922–33.
[14] Hu CQ, Zhang XZ, Huang SP. Class-E combined-converter by phase-shift control. In: 20th Annual IEEE Power Electronics Specialists Conference, Milwaukee, Wisconsin, USA, 26-29 June 1989. p. 229–234.
[15] Saito S, Mita S, Onishi H, Nagaoka S, Uematsu T, Sekiya H. Frequency-controlled resonant converter with push-pull Class-E inverter. In: 2019 IEEE Applied Power Electronics Conference and Exposition (APEC), Anaheim, California, USA, 17-21 March 2019. p. 1635–40.
[16] Yusop Y, Saat S, Nguang SK, Husin H, Ghani Z. Design of capacitive power transfer using a class-E resonant inverter. J Power Electron 2016;16(5):1678–88.
[17] Li YF, Tseng CS. Tracking control of class E inverter for the duty cycle control. In: 2014 IEEE 23rd International Symposium on Industrial Electronics (ISIE), İstanbul, Turkey, 1-4 June 2014. p. 2643-7.
[18] Koizumi H, Kurokawa K. Analysis of the class DE inverter with thinned-out driving patterns. IEEE Trans Ind Electron 2007;54(2):1150–60.
[19] Fujii M, Suetsugu T, Shinoda K, Mori S. Class-E rectifier using thinned-out method. IEEE Trans Power Electron 1997;12(5):832–6.
[20] Suetsugu T. Frequency characteristics of class E rectifier using thinned-out method. In: Proceedings of 40th Midwest Symposium on Circuits and Systems. Dedicated to the Memory of Professor Mac Van Valkenburg, Sacramento, California, USA, 6 Aug. 1997. p. 114-8.
[21] Öncü S, Sazak BS. Power control of single switch inverter with deleting some control pulses. J Fac Eng Arch Gazi Univ 2006;21(1):123–7.
[22] Fujita H, Akagi H. Control and performance of a pulse-density-modulated series-resonant inverter for corona discharge processes. IEEE Trans Ind Appl 1999;35(3):621–7.

[23] Leung HY, McCormick D, Budgett DM, Hu AP. Pulse density modulated control patterns for inductively powered implantable devices based on energy injection control. IET Power Electron 2013;6(6):1051–7.
[24] Li H, Fang J, Chen S, Wang K, Tang Y. Pulse density modulation for maximum efficiency point tracking of wireless power transfer systems. IEEE Trans Power Electron 2018;33(6):5492–501.
[25] Oncu S, Karafil A. Pulse density modulation controlled converter for PV systems. Int J Hydrogen Energy 2017;42(28):17823–30.
[26] Borekci S. Dimming electronic ballasts without striations. IEEE Trans Ind Electron 2009;56(7):2464–8.
[27] Sensui T, Koizumi H. Load-independent class E zero-voltage-switching parallel resonant inverter. IEEE Trans Power Electron 2021;36(11):12805–18.
[28] Kaczmarczyk Z, Jurczak W. A push–pull class-E inverter with improved efficiency. IEEE Trans Ind Electron 2008;55(4):1871–4.
[29] Zhang L, Ngo K. A constant-current ZVS class-E inverter with finite input inductance. IEEE Trans Ind Electron 2021;68(8):7693–6.
[30] Roslaniec L, Jurkov AS, Al Bastami A, Perreault DJ. Design of single-switch inverters for variable resistance/load modulation operation. IEEE Trans Power Electron 2015;30(6):3200–14.
[31] Issi F, Kaplan O. Design and application of wireless power transfer using Class-E inverter based on adaptive impedance-matching network. ISA Trans 2022;126:415–27.
[32] Shigeno A, Koizumi H. Half-wave class DE low dv/dt rectifier using thinned-out method with delta-sigma modulation. In: 2017 IEEE Energy Conversion Congress and Exposition (ECCE), Cincinnati, OH, USA, 1-5 Oct. 2017. p. 5638–44.
[33] Koizumi H, Sekiya H, Matsuo M, Mori S, Sasae I. Resonant DC/DC converter with class DE inverter and class E rectifier using thinned-out method (deleting some of the pulses to the rectifier). IEEE Trans Circuits Syst I: Fundam Theory Appl 2001;48(1):123–6.
[34] Kazimierczuk MK, Czarkowski D. Resonant power converters. New York, NY, USA: John Wiley & Sons; 2012.
[35] Yeon JE, Cho KM, Kim HJ. A 3.6 kW single-ended resonant inverter for induction heating applications. In: 2015 17th European Conference on Power Electronics and Applications (EPE'15 ECCE-Europe), Geneva, Switzerland, 8-10 Sept. 2015. p. 1-7.
[36] Karafil A, Ozbay H, Oncu S. Comparison of regular and irregular 32 pulse density modulation patterns for induction heating. IET Power Electron 2021;14(1):78–89.

Akif Karafil was born in Bursa, Turkey, in 1983. He received the B.S. degree in Electrical Education from Marmara University, İstanbul, Turkey, in 2007, the M.S. degree in Electrical and Electronics Engineering from Karadeniz Technical University, Trabzon, Turkey, in 2011, and the Ph.D. degree in Electrical and Electronics Engineering from Karabuk University, Karabuk, Turkey, in 2018. He is working at Yalova University Engineering Faculty, Department of Electrical and Electronics Engineering, Yalova, Turkey, where he is currently an Assistant Professor. His research interests include pulse density modulation control, resonant converters, soft switching, MPPT, single-phase grid-connected inverters, and PV system applications.